# Microfabricated hinges

# K. S. J. Pister

EECS Robotics Laboratory, 207-108 Cory Hall, Department of Electrical Engineering and Computer Sciences, University of California, Berkeley, CA 94720 (USA)

### M. W. Judy

Berkeley Sensor and Actuator Center, Department of Electrical Engineering and Computer Sciences, University of California, Berkeley, CA 94720 (USA)

# S. R. Burgett and R. S. Fearing

EECS Robotics Laboratory, Department of Electrical Engineering and Computer Sciences, University of California, Berkeley, CA 94720 (USA)

(Received September 12, 1991; accepted March 4, 1992)

#### Abstract

A new surface micromachining process has been developed for the fabrication of a wide variety of three-dimensional structures. Polysilicon structures with integrally fabricated hinges are rotated out of the plane of the wafer after fabrication, and interconnected with other structures to form complex three-dimensional designs with detailed features in all three dimensions. Electrical contact to the assembled structures has been demonstrated. Several structures are presented here: a hot-wire anemometer, a tissue growth dynamometer, and a gripper.

Keywords: surface micromachining, micromechanics, microhinges, three-dimensional structures, polysilicon.

#### 1. Introduction

Many sensor and actuator applications require three-dimensional components. A rich variety of processing techniques is used to fabricate these components: isotropic and anisotropic wet etching [1], deep plasma etching [2], specialized lithography [3], and laser-chemical methods [4]. Several conventional macro-scale processing techniques have also been adapted for use on the micro scale, including electroplating (e.g., LIGA [5]), electron discharge machining (EDM) [6], extrusion [7], and post-process assembly, such as wafer bonding [8].

Important characteristics of a three-dimensional fabrication process are the resolution in the plane of the wafer, resolution in the direction normal to the surface of the wafer, and range of feature size in these directions. We consider conventional lithographic techniques (i.e., those capable of producing distinct adjacent features on the order of 1 µm in size) to be the standard for 'high resolution'. It is important to distinguish between resolution and range. For example, with a given process it may be possible to obtain very accurate depth of

etch over the range  $1-500 \mu m$ , but difficult to have an adjacent feature of a different depth. This would be considered low resolution in the vertical (normal to the surface) direction.

With these characteristics in mind, we examine the processing techniques mentioned above. Wet etching of single-crystal silicon allows a very large range (from angstroms to millimeters) of vertical features to be fabricated, but the resolution of features on the surface is compromised as the depth of the etch is increased. Some control of vertical resolution is possible with dopant-sensitive etching, self-stopped anisotropic etching, and clever mask design, but in general the vertical resolution of wet etches is poor. In addition, the shape of the sidewalls of the etched regions is generally curved (isotropic etching), vertical (e.g., anisotropic etching of (110) silicon), or inclined at 54.74 degrees from the wafer surface (e.g., anisotropic etching of (100) silicon). Subsequent lithography is often complicated by the presence of large openings on either surface of the wafer.

Plasma etching also generates large vertical features, with substantially more flexibility and planar

resolution than wet etching, but the vertical resolution is even more limited than with wet etching. Some variation of sidewall angle is possible by varying the isotropy of the etch, but sidewalls are usually restricted to being either isotropic or nearly vertical. As with wet etching, large vertical sidewalls can make subsequent lithography more difficult.

X-ray lithography coupled with electroplating offers large vertical features and fine planar resolution, but, even with the use of sacrificial layers, has very poor vertical resolution. EDM and laser—chemical machining offer the widest variety of realizable geometries, with fine resolution in all dimensions, but suffer from limited throughput due to the sequential (rather than parallel) nature of the processes.

Standard surface micromachining, in contrast with the methods mentioned above, has high planar resolution, low vertical resolution, and limited vertical range (typically less than 5 µm). These characteristics make surface micromachining an excellent choice for planar applications, but have limited utility for three-dimensional designs. We present a process in which structures are fabricated using surface micromachining, and then rotated out of the plane of the wafer on integrally fabricated hinges (Fig. 1). The resulting structures have high resolution in both the planar and vertical directions, and have a vertical range from 10 µm to more than a millimeter. This hinge-based method allows the benefits of high-resolution surface lithography while providing access to the third dimension with

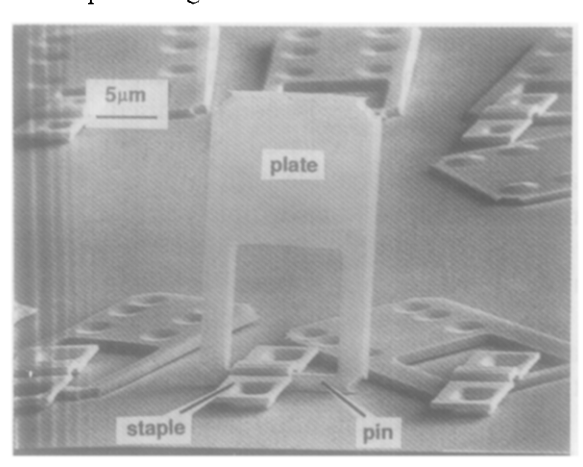
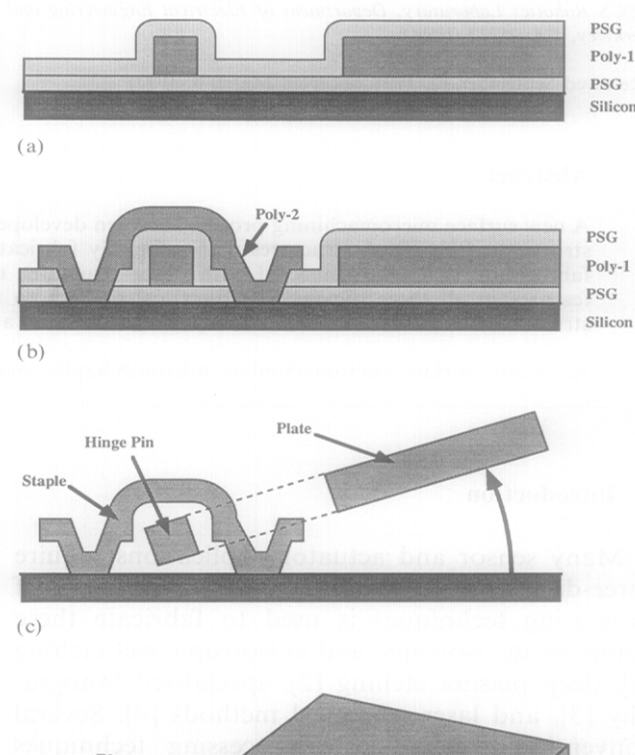


Fig. 1. An electron micrograph of an array of hinged plates. The central (vertical) plate is 40  $\mu$ m square. The vertical plate was already in this position after the post-release rinse, and did not require manual assembly. Dimples are visible on the top and bottom surfaces of several plates.

higher vertical resolution than previously possible. The drawbacks of hinge-based designs include the need for post-process assembly, and incompatibility with typical MOS processes.

#### 2. Process

The simplest version of the hinge fabrication process is a three-mask double-layer polysilicon process with oxide sacrificial layers (Fig. 2). A



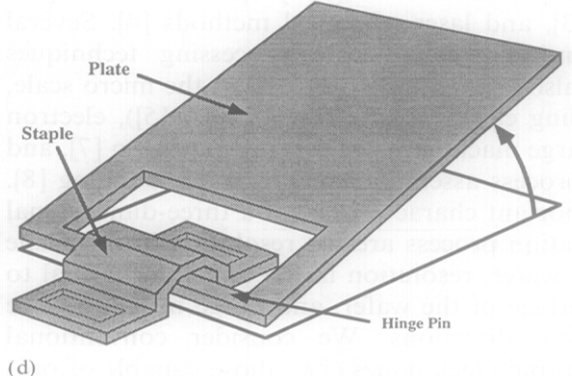


Fig. 2. A cross section of a simple hinge during fabrication. (a) The first PSG is deposited, poly-1 is deposited and patterned, and the second layer of PSG is deposited. (b) Contacts are etched through both layers of PSG. Poly-2 is deposited and patterned. (c) The oxide is removed in a sacrificial etch, and the poly-1 layer is free to rotate out of the plane of the wafer. (d) A perspective view of a hinged plate after release.

sacrificial phosphosilicate glass (PSG) layer is deposited on a bare substrate, followed by an undoped polysilicon layer (poly-1), and a doping PSG layer. All depositions are by low-pressure chemical vapor deposition (LPCVD). The resulting oxide/poly/oxide sandwich is annealed at 950 °C in a nitrogen ambient for one hour to reduce vertical stress gradients in the polysilicon, while doping the film at the same time. The top oxide is removed in 5:1 buffered hydrofluoric acid (BHF), and the polysilicon is patterned in a LAM model 480 plasma etcher using CCl<sub>4</sub>, helium, and oxygen. This polysilicon etch defines the majority of the structural components, including the hinge 'pins', about which most structures will rotate. A second sacrificial PSG is deposited (Fig. 2(a)) and both the first and second sacrificial oxides are patterned in a LAM model 590 plasma etcher using CF<sub>4</sub>, CHF<sub>3</sub>, and helium. This etch defines contacts between the second polysilicon layer and the substrate, as well as contacts between the two polysilicon layers. A second layer of polysilicon (poly-2) is deposited, covered with a second doping oxide, and annealed, as with poly-1. The doping oxide is removed and the polysilicon is patterned (Fig. 2(b)). This second polysilicon etch defines the 'staples' which tie the first polysilicon layer to the substrate, as well as forming additional structural components. Finally, the sacrificial layers are removed in a one minute concentrated (49%) HF etch, the wafers are rinsed in deionized water, and air dried at room temperature (Fig. 2(c,d)). Perforations are used in the larger structures to allow complete release in the one minute release etch (e.g., Fig. 5).

Typical film thicknesses for the sacrificial and doping PSG layers are between 0.5 and 2.5  $\mu$ m. Polysilicon layers are typically between 1 and 2  $\mu$ m thick. If the structures are intended to be electrically active (e.g., the anemometers discussed below), the substrate is passivated with a 0.5  $\mu$ m thermal oxide and 0.1  $\mu$ m LPCVD nitride before the first sacrificial oxide is deposited.

Dimples can be added to the polysilicon layers by patterning part way through the sacrificial layers with BHF. These dimples are not strictly necessary, but help prevent the polysilicon layers from adhering to the substrate and to each other after release. If a dimple etch is desired, it is important to anneal the PSG before the etch to ensure a uniform etch rate. Portions of poly-1 can be anchored to the

substrate, if desired, by etching contacts in the first sacrificial PSG before the poly-1 deposition.

Since the polysilicon etches are quite anisotropic, there are often 'stringers' left after the second polysilicon etch. Stringers are formed in areas where the second polysilicon film crosses over a vertical step (in this case, any edge of the first polysilicon layer). This vertical step results in a much thicker (vertically) poly-2 film near the step. When poly-2 is patterned in an anisotropic etch, only part of the thicker film is etched, leaving a thin stringer near every poly-1 edge. Stringers are undesirable because they get in the way during assembly (and tend to break off and land in inopportune places). They can be removed with either a wet or dry isotropic etch.

If the total thickness of the two sacrificial oxide layers is greater than the thickness of the first polysilicon layer, then the pin of the hinge will be able to slide between the two legs of the poly-2 staple (as in Fig. 1). This sort of 'play' in the hinge is not generally desirable, and can be eliminated by using a timed BHF etch immediately following the patterning of poly-1. This timed etch undercuts the sacrificial oxide under the hinge pin, and due to the poor step coverage of low-temperature LPCVD oxide, indirectly reduces the second sacrificial oxide thickness near the pin as well. This results in a partially encased poly-1 pin, under (and almost inside) a poly-2 staple. Since the hinge location is now determined by the poly-1 pin rather than the poly-2 staple contacts, we refer to this as a 'self-aligned' pin. Figure 3 shows a cross

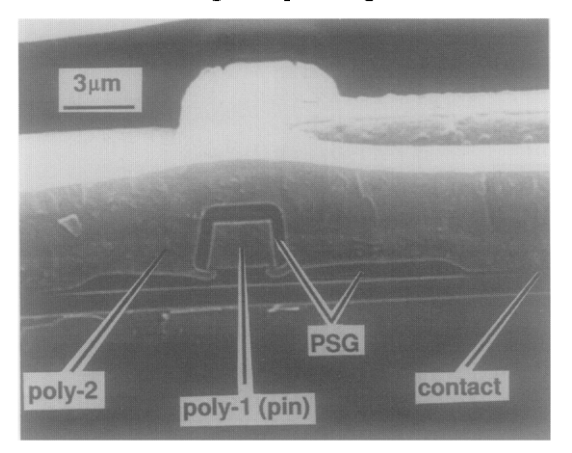


Fig. 3. An electron micrograph of a cross section through the pin of a substrate hinge. The small square in the center of the Figure is the poly-1 pin. Surrounding that is the poly-2 staple (covered with photoresist). Note the poly-2 to substrate contacts at either edge of the Figure. Also note small barbs of poly-2 which protrude slightly under the pin. This is a result of the self-aligning process.

section of such a self-aligned hinge pin after the poly-2 etch and before the final release etch.

# 3. Design

Given the three mask process above, it is possible to make several different types of hinges, as illustrated in Fig. 4. The simplest of these is the 'substrate hinge', shown in Figs. 1, 2, and 4(a), which consists of a poly-1 plate and hinge pin constrained by a poly-2 staple. The staple is attached to the substrate at two contact points, and the plate is free to rotate a full 180 degrees off the substrate. Note that the freedom of the plate to rotate may be limited by the geometry of the pin and staple. If the width of the pin is greater than the sum of the thicknesses of the poly-1 and sacrificial oxide layers, then the pin will be unable to rotate a full 90 degrees without contacting the substrate and staple.

The substrate hinge is used to hinge poly-1 plates to the substrate. To hinge plates to each other requires a different type of hinge. Two poly-1 plates can be hinged together using a 'scissor hinge', as shown in Fig. 4(b). Poly-2 strips are attached between interdigitated poly-1 fingers, preventing the two poly-1 plates from pulling apart, and allowing the plates a relative rotation of roughly 180 degrees. This type of hinge can only fold 'concave-down'. A similar scissor hinge, illustrated in Fig. 4(c), hinges two poly-2 plates together and folds 'concave-up'. Another style of scissor hinge

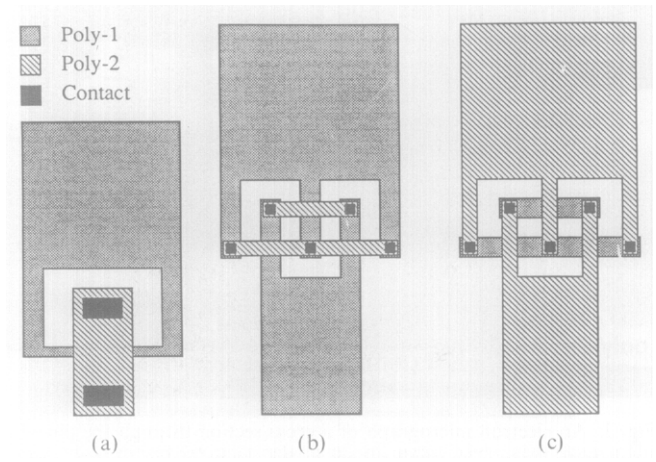


Fig. 4. Three basic hinge types. (a) A substrate hinge, which is used to hinge released structures to the substrate. (b) A 'concave down' scissor hinge, used to hinge released structures to each other. (c) A 'concave up' scissor hinge.

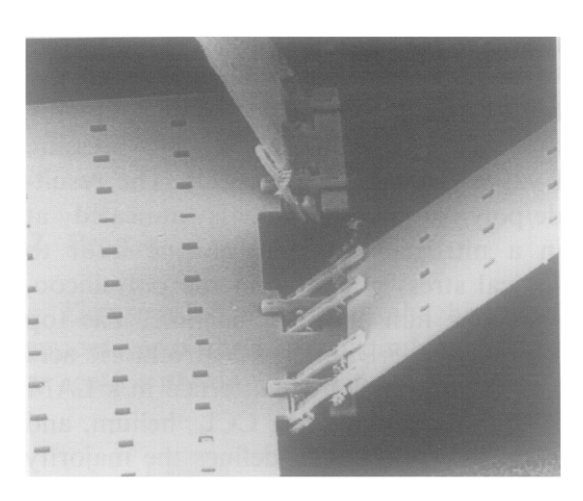


Fig. 5. An electron micrograph of poly-1 plates hinged together with scissor hinges. The smaller plates are  $100 \mu m$  wide. Large structures such as these are usually designed with  $2-5 \mu m$  perforations to reduce the length of the release etch.

allows two poly-1 plates to be attached with a concave-up hinge, as shown in Fig. 5.

Unlike substrate hinges, there is no 'pin' in a scissor hinge. Given the typical film thicknesses used, a substrate hinge which is intended to rotate 90 degrees must have a pin no more than  $2 \mu m$  wide. Scissor hinge geometries are not constrained by the film thickness of the structural or sacrificial layers. As a result, scissor hinges can be made with all geometries much wider than  $2 \mu m$ , making them much stronger than substrate hinges.

### 4. Assembly

After the release etch, the structures are rotated into their final positions. This is currently accomplished at a probe station using standard electrical probing equipment to rotate the structures into position. A sharp probe tip is slid under a released structure and raised to lift the structure off the surface of the wafer and rotate it into the desired position. By interlocking two hinged structures, as shown in Figs. 6 and 10, the final position of the structures can be accurately controlled. The hinges can be permanently locked into position by an additional deposition step. For example, a 0.3 µm PECVD oxide deposited on assembled structures enables substrate hinges to withstand torques in excess of 10 nN m (=1 milligram force at 1 millimeter) without damage.

Assembly is a labor-intensive process (e.g., the gripper requires roughly 10 minutes for assembly),

however, we are working on designs that require no manual assembly. Hydrodynamic forces may prove to be very useful in automating the assembly process. We have observed that many structures rotate 90 degrees or more during the post-release rinse, and a directed stream of air from a capillary tube has a similar effect on released structures. Experiments have shown that depositing a tensile film (e.g., 0.1 µm sputtered molybdenum,  $1.5 \times 10^{11}$  Pa tensile stress) on the post-release structures makes them much more susceptible to hydrodynamic forces, due to the resulting curvature of the plates. We hope to exploit this behavior by designing structures that will have a tendency to 'snap' into place when they are close to their desired final positions. In this way, an entire wafer could be batch assembled by vigorous agitation in a DI rinse, or individual structures could be assembled sequentially using directed streams of air.

#### 5. Results and discussion

With one exception (the gripper) the devices presented here do not use the hinges for active rotation. Rather, the hinges are used only during assembly to rotate the structure into position. Thereafter, the hinges are designed to remain locked in place. Motion of the structures is then obtained by using the bending of beams. In this way, the high friction of the hinges is an advantage during assembly, and is not a hindrance during use. With these ideas in mind, we present a few examples of hinged structures.

### 5.1. Hot-wire anemometer

A wide variety of micromachined anemometers, including polysilicon hot-wire anemometers, appears in the literature [9-11]. A common theme in these designs is the desire for low thermal mass and high thermal isolation to improve response time and sensitivity. Most designs place the active portion of the anemometer within a few microns of the substrate, or etch a cavity beneath it. We hope to improve on the sensitivity and response time of these designs by placing the hot wire several hundreds of microns above the substrate, thereby achieving thermal isolation and increased exposure to the fluid flow.

Figure 6 shows a 200 μm long, 2 μm wide polysilicon 'hot wire' which is suspended between

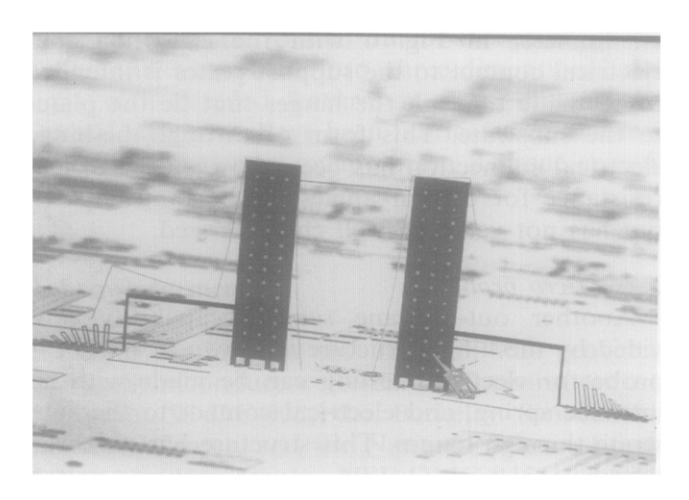


Fig. 6. A single-axis hot-wire anemometer. The supports are  $100 \, \mu m$  by  $400 \, \mu m$  tall, and the wire is  $2 \, \mu m$  wide and  $200 \, \mu m$  long. The right support is locked in the vertical position by the smaller hinged structure at its base. Serpentine springs to either side of the supports guarantee electrical connection to the erected structure. Note the stringers visible around the supports.

two hinged plates. Electrical contact to each side of the hot wire is supplied from a surface bonding pad through a serpentine spring to the support plate. An initial characterization of this structure was performed by passing a current through the device while directing the air flow from a 0.5 mm diameter tube across the wire. The results indicate a repeatable monotonic dependence of resistance on flow rate.

Figure 7 shows an as yet untested three-axis anemometer. This device is similar to the

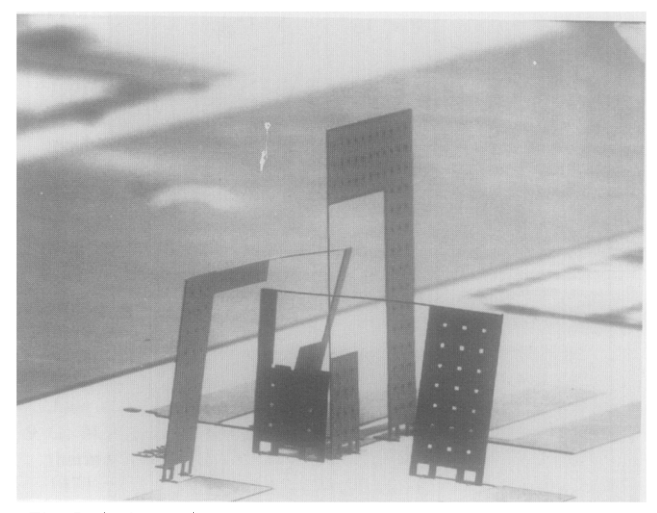


Fig. 7. A three-axis anemometer. The wires are  $2 \mu m$  by  $2 \mu m$  by  $200 \mu m$  and all pass within  $50 \mu m$  of a single point. Three orthogonal wires should give enough information to determine both the magnitude and direction of fluid flow in three dimensions.

anemometer in Fig. 6 with the exception that electrical contact to the support plates is intended to be made through the hinges that tie the plates to the substrate. This form of through-the-hinge electrical connection has been shown to be of low resistance for certain angles of the hinged plate, but has not yet been well characterized.

### 5.2. Micro probe

Another out-of-plane sensing capability provided by the hinge structure is shown in Fig. 8. A probe for electrical testing can be made with an intrinsic spring, and electrical contact to the substrate through hinges. This structure has not been tested.

# 5.3. Tissue-growth dynamometer

The device shown in Fig. 9 measures the forces exerted by growing embryonic tissue. In this particular application, a sub-millimeter piece is dissected from a growing frog embryo and placed inside the central enclosure, which is submerged in a nutrient solution. As the tissue grows, the sides of the box are pushed out, and the deflection is monitored visually with a microscope and a time-lapse recording system. Each side of the box is composed of a free (not attached directly to the substrate) vertical plate that is supported by beams which extend back to a fixed vertical plate. Deflection is measured using a row of 2 µm lines/spaces

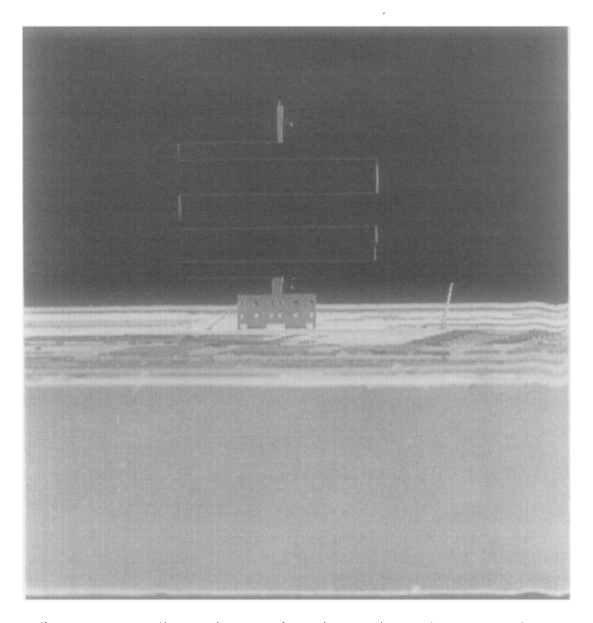


Fig. 8. A compliant micro probe. The total length of the spring is 3 mm.

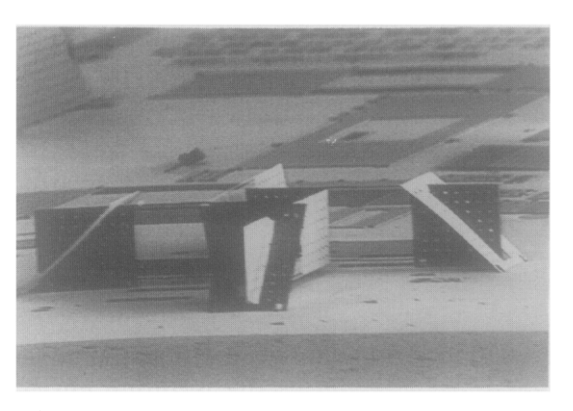


Fig. 9. SEM of a box which measures the forces exerted by developing embryonic tissue. A growing tissue sample placed in the central open area causes the inner plates to deflect. Deflection is measured visually to determine applied force. Vertical plates are 200 μm square, beams are 200 μm long.

fabricated on the edges of the support beams. By varying the dimensions of the plates and beams it is possible to accommodate a wide variety of tissue-sample sizes, and a large range of forces. Devices fabricated and assembled to date range from plate dimensions of 0.1 mm to 0.5 mm, and beam lengths from 0.1 mm to 1.0 mm. This translates to a range of measurable forces from 0.1 nN to  $10 \,\mu\text{N}$ . Experiments have shown that tissue samples do not appear to be adversely affected by the presence of the box. Preliminary results show that growing embryonic spinal cord samples can exert a force of 50 nN on a 300  $\mu$ m square plate.

# 5.4. Parallel-plate gripper

Recently, planar (roughly 2  $\mu$ m thick) microgrippers have been fabricated with a gripping range on the order of 10  $\mu$ m [12, 13]. The hinge technology offers the opportunity to produce micro-grippers of a scale difficult to obtain with previous micromachining processes. Grip-surface dimensions and gripper openings measured in hundreds of microns are possible, while actuating resolution is on the order of microns.

The structure in Fig. 10 is a parallel-plate gripper consisting of four separate pieces. The two jaws of the gripper are folded up separately and locked in place at one end by another plate with two slots in it. The jaws are suspended at the end of 400  $\mu$ m long beams, each of which is 20  $\mu$ m wide. A 1 mm long tendon travels from each jaw and locks into the vertical handle. When the handle is pulled back, the tendons pull the jaws open. When the handle is released, the spring force of

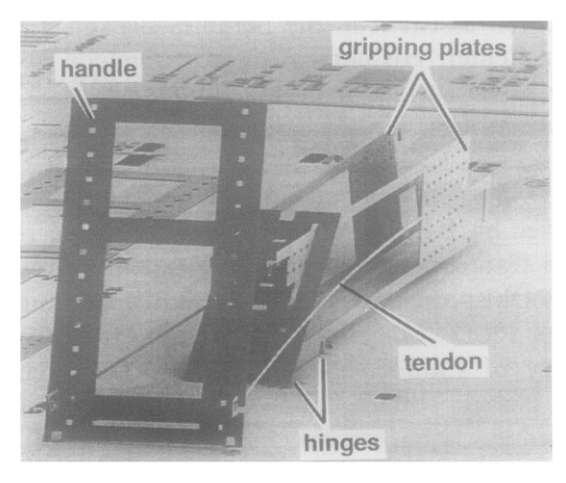


Fig. 10. A parallel plate gripper. The gripper is normally closed, with a gap of  $100 \,\mu m$  between the plates. Pulling the vertical bar (left side) causes the jaws to open. Opening of 0.5 millimeter is possible with no damage to the device.

the support beams closes the jaws. In the 'closed' (rest) position the jaws are actually  $100 \, \mu m$  apart. Over 100 cycles of up to  $0.5 \, mm$  opening have caused no damage to the gripper.

This method of actuating the gripper demonstrates that it is possible to couple mechanically off-chip actuators with on-chip structures. The handle provides a reduction of roughly ten to one from the motion of its top to the motion of the tendons. Thus a travel of about half a millimeter at the top of the handle opens the jaws fully. A fixture has been built which allows an operator to exercise the gripper by turning a 32 thread-perinch screw. A 25 µm aluminum bonding wire is threaded through the handle and bent back to secure it. Axial motion of the screw is transmitted to the bonding wire, giving full range of motion of the gripper for approximately one turn of the screw. To provide x, y, and z positioning of the gripper, the fixture mates to a standard three-axis micromanipulator mount in a probe station.

#### 6. Conclusions

A new surface micromachining process has been developed which allows a wide variety of three-dimensional structures to be fabricated. The three-mask process allows structures to be hinged to the substrate as well as to each other. By fabricating the structures in the plane of the wafer, conventional lithographic techniques can be used to define features with high resolution. These struc-

tures can then be rotated out of the plane of the wafer and assembled into three-dimentional designs with detailed features in three dimensions. Several structures have been fabricated and tested, including a hot-wire anemometer, a tissue-growth dynamometer, and a gripper.

# Acknowledgements

Partial funding for this research was provided by the Semiconductor Research Corporation under grant 91-DC-008, the Berkeley Sensor and Actuator Center, and the National Science Foundation under grants NSF-DMC-8451129 and NSF-ECS-8719298. Many thanks to the staff of the Berkeley Microfabrication Facility. We greatly appreciate the advice and encouragement of R. S. Muller.

#### References

- 1 K. E. Peterson, Silicon as a mechanical material, *Proc. IEEE*, 70 (1982) 420-457.
- 2 M. Zdeblick, P. Barth and J. Angell, Microminiature fluidic amplifier, Proc. IEEE Solid State Sensors Workshop, Hilton Head Island, SC, USA, June 2-5, 1986.
- 3 W. E. Feely, Micro-structures, Proc. IEEE Solid State Sensor and Actuator Workshop, Hilton Head Island, SC, USA, June 6-9, 1988, pp. 13-15.
- 4 T. Bloomstein and D. Ehrlich, Laser-chemical three-dimensional writing of multimaterial structures for microelectromechanics, *Proc. IEEE Micro Electro Mechanical Systems Workshop, Nara, Japan, Jan. 30-Feb. 2, 1991*, p. 202.
- 5 J. Mohr, P. Bley, C. Burbaum, W. Menz and U. Wallrabe, Fabrication of microsensor and microactuator elements by the LIGA-process, Proc. 6th Int. Conf. on Solid-State Sensors and Actuators (Transducers '91), San Francisco, CA, USA, June 24-28, 1991, pp. 607-609.
- 6 T. Masaki, K. Kawata and T. Mauzawa, Micro electro-discharge machining and its applications, Proc. IEEE Micro Electro Mechanical Systems Workshop, Napa, CA, USA, Feb. 11-14, 1990, pp. 21-26.
- 7 S. Jacobson, R. Price, J. Wood, T. Rytting and M. Rafaelof, The wobble motor: an electrostatic, planetary-armature, microactuator, Proc. IEEE Micro Electro Mechanical Systems Workshop, Salt Lake City, UT, USA, 1989, pp. 17-24.
- 8 W. Henrion, L. DiSanza, M. Ip, S. Terry and H. Jerman, Wide dynamic range direct digital accelerometer, Proc. IEEE Solid State Sensor and Actuator Workshop, Hilton Head Island, SC, USA, June 4-7, 1990, pp. 153-157.
- 9 G. N. Stemme, A monolithic gas flow sensor with polyimide as thermal insulator, *IEEE Trans. Electron Devices*, ED-33 (1986) 1470-1474.
- 10 M. Parameswaran, A. Robinson, L. Ristic, K. Chau and W. Allegretto, A CMOS thermally isolated gas flow sensor. Sensors Mater., 2 (1990) 17-26.
- 11 C. Mastrangelo and R. Muller, A constant-temperature gas flowmeter with a silicon micromachined package, Proc. 4th Int.

- Conf. Solid-State Sensors and Actuators (Transducers '87), Tokyo, Japan, June 2-5, 1987, pp. 43-47.
- 12 L. Chen, Z. Zhang, J. Yao, D. Thomas and N. MacDonald, Selective chemical vapor deposition of tungsten for microdynamic structures, *Proc. IEEE Micro Electro Mechanical Systems Work-shop*, Salt Lake City, UT, USA, 1989, pp. 82-87.
- 13 C. Kim, A. Pisano, R. Muller and M. Lim, Polysilicon microgripper, Proc. IEEE Solid State Sensor and Actuator Workshop, Hilton Head Island, SC, USA, June 4-7, 1990, pp. 48-51.

# **Biographies**

Kristofer S. J. Pister received his M.S. in electrical engineering from the University of California, Berkeley in 1989, and his B.A. in applied physics from the University of California, San Diego in 1986. He is currently a doctoral candidate in electrical engineering at University of California, Berkeley. His research interests include microrobotics, biomedical applications of robotics, and control theory. His e-mail address is kpister@diva.berkeley.edu.

Michael W. Judy was born in Minnesota in 1965. He received his S.B. degree in electrical engineering at the Massachusetts Institute of Technology in 1987. He is currently a Ph.D. candidate at the University of California, Berkeley, working

as a research assistant in the Berkeley Sensor and Actuator Center. His current interests include developing novel surface micromachining processes. His e-mail address is judy@diva.berkeley.edu.

Steve R. Burgett was born in Oklahoma in 1962. He received his B.S. degree in mechanical engineering from California Polytechnic State University, San Luis Obispo in 1987. He is currently working toward a Ph.D. in electrical engineering at the University of California, Berkeley. His research interests include robotics and control theory. His e-mail address is burgett@robotics.berkeley.edu.

Ronald S. Fearing received the S.B. and S.M. degrees from Massachusetts Institute of Technology, Cambridge, MA, in 1983. He earned the Ph.D. in electrical engineering at Stanford University, with a thesis in the area of robotic tactile sensing. He has been at the Electrical Engineering and Computer Sciences Department at the University of California, Berkeley, since January 1988, where he is currently an assistant professor. He received the Presidential Young Investigator Award in 1991. His research interests are in tactile sensing, dextrous manipulation, micro-robots and natural intelligence.